THE JOURNAL OF PHYSICAL CHEMISTRY C

Article

Disclosing the Early Stages of Electrochemical Anions Intercalation in Graphite by a Combined AFM/STM Approach

Gianlorenzo Bussetti, Rossella Yivlialin, Dario Alliata, Andrea Li Bassi, Chiara Castiglioni, Matteo Tommasini, Carlo Spartaco Casari, Matteo Passoni, Paolo Biagioni, Franco Ciccacci, and Lamberto Duò

J. Phys. Chem. C, **Just Accepted Manuscript** • DOI: 10.1021/acs.jpcc.6b00407 • Publication Date (Web): 23 Feb 2016

Disclosing the Early Stages of Electrochemical Anions Intercalation in Graphite by a Combined AFM/STM Approach

Gianlorenzo Bussetti[1], Rossella Yivlialin[1], Dario Alliata[2], Andrea Li Bassi[3], Chiara Castiglioni[4], Matteo Saverio Tommasini[4], Carlo Spartaco Casari[3], Matteo Passoni[3], Paolo Biagioni[1], Franco Ciccacci[1], Lamberto Duò[1]*

1) Department of Physics, Politecnico di Milano, p.za Leonardo da Vinci 32, I-20133, Milano (Italy).

2) Rudolph Technologies, Inc. Bloomington MN, U.S.A.

3) Department of Energy, Politecnico di Milano. v. Ponzio 34/3, I-20133, Milano (Italy).

4) Department of Chemistry, Materials and Chemical Engineering, Politecnico di Milano, p.za Leonardo da Vinci 32, I-20133, Milano (Italy).

Corresponding Author

* Corresponding Author e-mail: gianlorenzo.bussetti@polimi.it; tel.: +390223996181

Abstract. In view of large-scale applications, electrochemical exfoliation of graphite for the production of graphene sheets must follow chemical processes that ensure high quality of the

products, i.e. wide-size graphene foils, single- or few-layer thickness, low level of defectivity in order to guarantee high electrical transport and good mechanical properties. Understanding the exfoliation process of graphite at the atomic scale, e.g. the intercalation of graphene layers in the electrolyte solution, is fundamental in order to really be able to control and optimize such processes. This can be obtained for instance by investigation of the exfoliated graphite, i.e. the surface of the original crystal left behind in the chemical solution and by real time monitoring of the graphite surface morphological and structural modifications during the exfoliation process. Here, we monitor the graphite surface changes as a function of the electrochemical potential by both electrochemical (EC) atomic force microscopy and EC-scanning tunneling microscopy coupled with cyclic voltammetry. Following this strategy, we disclose the surface modifications encountered during the early stages of anion intercalation, for different electrolytes: surface faceting, step erosion, terrace damages, and nano-protrusions, all affecting the graphite surface and therefore the exfoliation process. Our results represent a key step towards a full investigation of the intercalation process in graphite. Within the current debate on the exfoliation of layered crystals, these data potentially represent important information for investigation of the intercalation process in graphite and, on the other hand, for further optimization of the electrochemical protocol for graphene production.

Keywords. Graphite exfoliation, electrochemical-AFM, electrochemical-STM, nano-protrusion formation, surface faceting, cyclic voltammetry.

Introduction.

The development of flat and flexible electronics, ultra-thin sensors and nano-electromechanical systems requires production and characterization of high quality ultra-thin films to be used as gates, electrodes, substrates, etc. In this context, layered crystals have recently attracted a growing interest, and a systematic research towards technological development of single or few-layer materials started about 10 years ago, when the graphene properties were clearly described[1,2]. With its electron mobility at room temperature 10 times higher than that of silicon, graphene is one of the most promising candidates for replacing Si, according to the International Technology Roadmap for Semiconductors[3]. A perspective regarding the 21-st century technology is to develop new protocols for exfoliating different layered crystals, besides graphite[4]. Flexible electronics, sensors, energy conversion devices, telecommunications, light and robust mechanical structures and medical applications require the production of large amounts of good quality, large sheets via ecologically compatible protocols. A currently widely investigated approach is that of developing suitable chemical strategies[5], i.e. the so-callled liquid exfoliation. Unfortunately, evidence is still missing that every layered crystal can be chemically exfoliated, which represents a bottleneck for further developments[3]. In this respect, graphite and graphene are representative systems to test hypotheses, apply experimental strategies and check exfoliation protocols that can be in principle extended to other layered crystals. However, the lack of a complete and detailed knowledge of the microscopic mechanisms occurring at the

graphite surface during exfoliation makes this challenge even more complex. Recently, an original approach to fill this information gap was proposed by Xia *et al.*[6]. The authors focused their attention on the crystal (graphite in their study) left inside the solution, after the exfoliation process, rather than on the produced sheets (here graphene). To this purpose, an electrochemical atomic force microscopy approach (EC-AFM) was employed. The EC-AFM is a technique able to observe the surface morphology when immersed inside the electrolytic solution under potentiostatic control. Originally, the EC-AFM was used in a pioneering investigation of the anion intercalation process in graphite, where the percolation of $(ClO_4)^-$ and $(SO_4)^{2-}$ below the crystal uppermost layer produces large (hundreds of nanometers) bubbles (called blisters) on the surface[7,8]. However, some important questions are still debated: what is the evolution of the crystal surface morphology at the very first stages of the intercalation process? Can the preferential paths of the acid ions during intercalation (i.e. defects and steps) be monitored and characterized in real time? Is there a progressive damage of the crystal surface during intercalation? What is the time scale of these processes? How does the surface morphology change as a function of the electrochemical potential applied on the sample? Answering these questions can prove useful for a further improvement and optimization of the chemical exfoliation processes, tuning the local surface dynamics at the first stages of anion intercalation. As a complementary characterization, the local morphology and the crystal structure can be explored by EC-scanning tunneling microscopy (EC-STM)[9,10,11,12,13,14], possibly achieving an atomic resolution imaging of the surface morphology. This set-up has been rarely applied to the case of anions intercalation[15,16,17], where the crystal surface is heavily modified and the high perturbing faradaic currents, flowing through the surface, make the EC-STM an uncommon technique for this kind of investigations.

In this paper, we address and answer some of the aforementioned questions by means of an analysis based on both EC-AFM and EC-STM coupled with cyclic voltammetry. Four different acid solutions [namely hydrochloric acid (HCl), perchloric acid ($HClO_4$), sulfuric acid (H_2SO_4) and phosphoric acid (H_3PO_4)] were used as model electrolytes to compare the surface morphology of a Highly Oriented Pyrolytic Graphite (HOPG) crystal when: i) no intercalation is induced (HCl); ii) blisters formation occurs ($HClO_4$ and H_2SO_4); iii) anions intercalation is expected without blisters on the surface (H_3PO_4)[18]. Despite perchloric and sulfuric acids are not the most performing electrolytes for graphite exfoliation, they represent common solvents to induce anions intercalation and blister formation. The collected results disclose a new phenomenology and surface dynamics of the very first stages of anion intercalation, which can play an important role to clarify the molecular mechanisms involved in the process. In addition, we demonstrate that EC-STM, coupled with cyclic voltammetry, can be performed during the intercalation, paving the road towards further investigations aimed at disclosing the fine details of the process.

Methods.

Z-grade highly oriented pyrolytic graphite (10x10 mm^2, Optigraph©) is used as working electrode (WE) inside a three-electrode electrochemical cell. The graphite was exfoliated by adhesive tape along an edge of the sample. The acid electrolyte solutions were purified by bubbling Ar gas (5.0 grade pure) inside a separator funnel for several days. A Pt wire was used as both the counter electrode (CE) and the reference electrode (RE). The latter shows an energy shift with respect to the normal hydrogen electrode (NHE). When Pt electrode is used in sulfuric

acid, the potential shift is +0.743 V. The CE and the RE were left inside the electrolyte solution for 24 hours before each experiment. The WE, CE and RE were connected directly to the bi-potentiostat. No separators were used in our electrochemical cell.

A commercial (5500 by Keysight© Technology) electrochemical atomic force microscope (EC-AFM), coupled with an EC-scanning tunneling microscope (EC-STM), was used in the experiment. The EC-cell was placed on the WE, where a Viton O-ring ensures the seal of the electrolyte solution. The AFM cantilever can be easily exchanged with the STM tip without perturbing the sample and the electrochemical solution. The EC-cell and the scanning probe microscope can be placed inside a protected Ar environment. AFM images were collected in contact mode. A Pt/Ir tip was used for the STM. The tip was protected by wax to reduce the faradaic currents. A bi-potentiostat allowed choosing the proper EC-potential applied on the tip with respect to the RE for minimizing the faradaic current on the tip. The applied STM V_{bias} was obtained as a difference between the sample (WE) and the tip electrochemical potentials.

When the sample was placed in the electrochemical cell, the WE was set to a potential where the faradaic current was close to zero. A fast CV scan of the tip as the function of the electrochemical potential was acquired to find the range where the faradaic currents on the tip were minimized, keeping fixed the WE potential. After determining the potential of the tip, the latter was approached to the WE.

Results & Discussion.

When HOPG is immersed in HCl 2M and the applied potential is controlled by a bipotentiostat, the surface is stable and the morphology is the same shown by AFM images acquired in air or vacuum: flat terraces and sharp edges are visible in the AFM image shown in Figure 1 panel a.

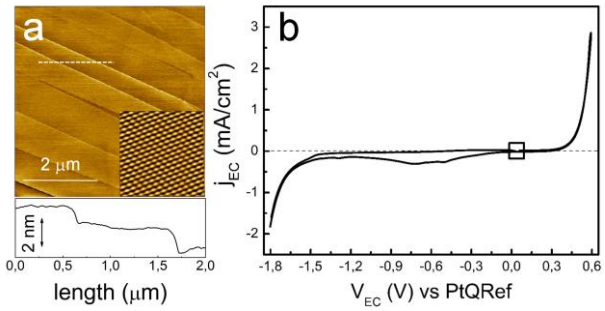

Figure 1. a) EC-AFM image (topography, contact mode) acquired on graphite immersed in HCl solution, after several electrochemical cycles. The atomic resolution [EC-STM (I_{tunnel} = 2 nA; V_{bias} = 0.3 V)] is reported in the inset (5 x 5 nm^2). At the bottom, scan profile of the graphite terraces along the white dotted line. b) Characteristic CV (scan rate v_{scan} = 100 mV/s) of graphite in HCl electrolyte. The square symbol marks the electrochemical potential (V_{EC}) value at which the EC-AFM and EC-STM images (of panel a) have been acquired. The V_{EC} value is measured with respect to a quasi-reference electrode (QRE), made of a Pt wire immersed inside the electrochemical solution, whose potential changes predictably with conditions.

By changing the scanning head, a STM acquisition is possible on the same sample in the same electrolyte solution under potential-controlled conditions. The high resolution STM image (see the inset in Figure 1, panel a) shows the typical atomic structure of the graphite surface, where atoms lie on a flat terrace. The absence of ion intercalation is consistent with the cyclic voltammogram (CV) shown in panel b. Here, no anodic (positive) peak is registered during the EC-potential scan. The small cathodic (negative) current, measured at around -0.7 V and due to reduction processes, is expected when the anodic sweeping is driven to oxidation potentials (here around 0.6 V).

The situation dramatically changes when graphite is immersed in $HClO_4$ 2M, which gives rise to anion (ClO_4^-) induced intercalation and blisters formation. When the sample is held at a suitable EC-potential (V_{EC} = 0.9 V), the AFM reveals blisters (observe the large bubbles in Figure 2a) after several minutes of a few consecutive cycles. Accordingly, the CV (panel b) shows a clear anodic peak at about 0.9 V, as reported in the literature[6]. This feature is related to the first of the

four expected stages of anions intercalation[7,8]. The difference between the areas (which represent the integrated charge) under the anodic and cathodic peaks (placed at 0.90 V and 0.83 V, respectively) suggests that a non-zero charge (of about 10 mC) has been stored in the sample.

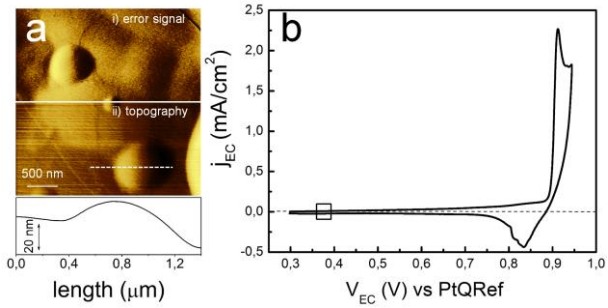

Figure 2. a) EC-AFM image [error signal (i) and topography (ii), contact mode] acquired on graphite immersed in 2M $HClO_4$ solution, after the anions intercalation and blister formation. At the bottom, scan profile of the blister. b) Characteristic CV (v_{scan} = 10 mV/s) of graphite in 2M $HClO_4$, acquired after the first sweep. The square symbol marks the value of the electrochemical potential at which the EC-AFM image (of panel a) has been acquired. For the definition of the PtQRef, electrode, see caption of Figure 1.

In Figure 3a, an EC-STM in plane raster scan is coupled with a CV half cycle: *each horizontal STM scan line* refers to a specific V_{EC} value, as specified in the CV on the left side. Despite an intrinsic difficulty in driving the STM tip during the CV acquisition, a precise and suitable change of the tip EC-potential (tens of mV) allowed us to obtain a real-time monitoring of the graphite surface morphology as a function of the V_{EC} applied on the sample. During the scanning, which starts at the bottom line of the map, V_{EC} is initially set to 0.3 V with respect to the Pt reference electrode and then gradually increased up to 1.0 V. A scan profile, reported at the bottom of the panel, shows graphite terraces, whose behavior is almost comparable with the terraces observed in Figure 1, suggesting a negligible role of the acid before the perchlorate ions intercalation. When the latter starts (maximum value of the faradaic current at V_{EC} = 0.9 V), the STM tip is slowly lifted off the surface, by lowering the tunneling current set-point, to avoid

instabilities during the scanning. The V_{EC} is then set at 0.3 V in such a way that the faradaic current decreases. When the STM acquisition starts again, the very first changes in the graphite morphology are observed (panel b).

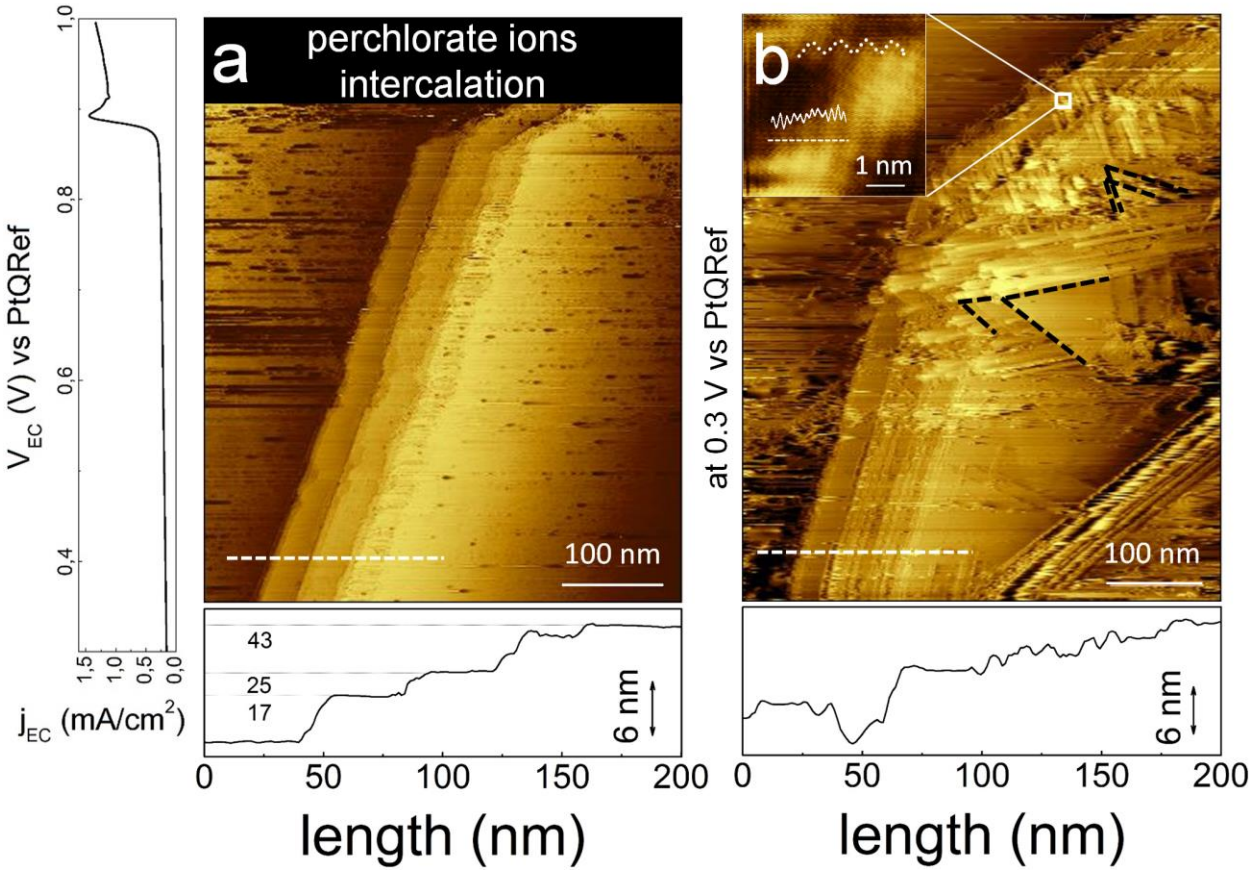

Figure 3. a) EC-STM image (I_{tunnel} = 0.2 nA) acquired on graphite immersed in $HClO_4$ solution. At the bottom, height profile of the graphite multi-atomic steps (17, 25 and 43 mono-atomic graphite layers) is reported. The graph on the left reports the CV sweep during the EC-STM scanning (see text for details). The "perchlorate ions intercalation" region takes few seconds to be covered during the completion of the bias sweep. The height profile taken along the dotted white line (bottom) shows flat terraces and sharp edges. b) EC-STM image (I_{tunnel} = 0.2 nA; V_{bias} = 0.3 V) acquired after the anions intercalation at fixed V_{EC} = 0.3 V. Preferential surface erosions, forming sharp 60° structures, are marked with black dashed lines. At the bottom, scan profile of the graphite terraces, where a significant increase of the surface roughness is observed. *Inset*: atomic resolution obtained on nano-protrusions. The dotted white line underlines the Moiré modulation super-imposed on the graphite lattice.

During intercalation, terraces are eroded (faceting) towards the steps, creating local damages on the surface (holes), new edges, terraces and vertices [forming angles of about 60° between adjacent terrace sides (see the black dashed lines in the figure)]. Accordingly, the scan profile (reported at the bottom of the panel) reveals a clear enhancement of the surface roughness. A closer inspection shows that the local morphology of the graphite terraces is perturbed (inset of panel b). Here, in fact, the atomic structure is still visible but atoms do not lie on a flat plane: nano-protrusions (brighter regions in the image), randomly spread on the surface, are clearly discernible. In addition, a Moiré pattern is visible (periodic modulation superimposed over the atomic resolution), suggesting that the acid intercalation has partially decoupled the uppermost graphite layers from the deeper ones. The nano-protrusions shape is essentially unchanged if the STM V_{bias} is tuned over about 700 mV by fixing the working electrode (WE) potential and modifying the tip electrochemical one. This suggests that nano-protrusions are mainly due to a topographic effect of the anions intercalation, as observed by the STM. The structure of these swellings is noteworthy. In Figure 4, the hexagonal geometry of the nano-protrusion surface lattice (panel a) has been studied by comparing the scan profiles acquired along i) a line parallel to the protrusion edge (dashed black line) and ii) a line crossing the protrusion (dotted red line) (panel b).

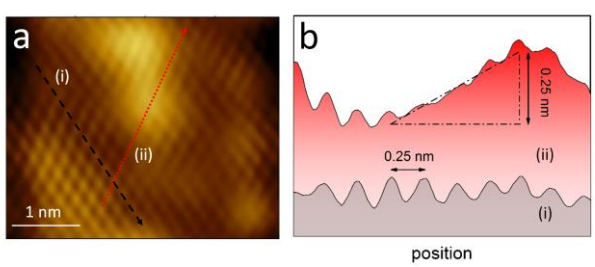

Figure 4. a) atomic resolution image of the nano-protrusion structure observed in $HClO_4$ solution [EC-STM image (I_{tunnel} = 0.7 nA; V_{bias} = 0.3 V)]. The dashed lines represent two different scan profiles: parallel to the protrusion edge [dashed black line

(i)] and cutting through the swelling [dotted red line (ii)]. b) scan profiles of the nano-protrusion. The distance between two corrugation maxima is almost unaffected by the surface swelling.

By comparing the two scan profiles, the C-C bond length inside the nano-protrusion is stretched by about 3%, as demonstrated with a simple geometric construction (see the triangle in panel b). This value is not negligible for a graphite surface but it is admissible in graphene sheets, as deduced from the mechanical properties of graphene[19,20,21,22]. In particular, structural swellings (called nanobubbles) comparable to these nano-protrusions on graphite have been recently observed at the graphene/Ir(100) interface, when sub-monolayers of Ar are intercalated inside the sample under vacuum conditions[23]. While in that case the authors give direct evidence that Ar gas is placed below the graphene sheet, in our working environment -provided by the electrochemical cell- the demonstration that the nano-protrusion encloses molecules of gases similarly to blisters (O_2, CO or CO_2, accordingly with the proposed model[24]) is challenging, despite a common origin (anions intercalation) between blisters and nano-protrusions,. Finally, we observe that both blisters (see Figure 2a) and nano-protrusions (see inset of Figure 3b and Figure 4a) do not show any morphological change after tens of tip scans.

The anions intercalation process starts close to surface defects, such as step edges[24]. If the EC-potential in the cell with the $HClO_4$ solution is set at a value slightly lower than 0.9 V, in order to keep a low enough anion intercalation rate, we observe that the graphite steps are increasingly smoothed and the edges eroded, as visible in Figure 5. In addition, we observe both formation and evolution of holes, which show a progressive broadening within a few minutes. This phenomenology is critical because, during the graphene production, the flake size is influenced by the quality of the graphite surface.

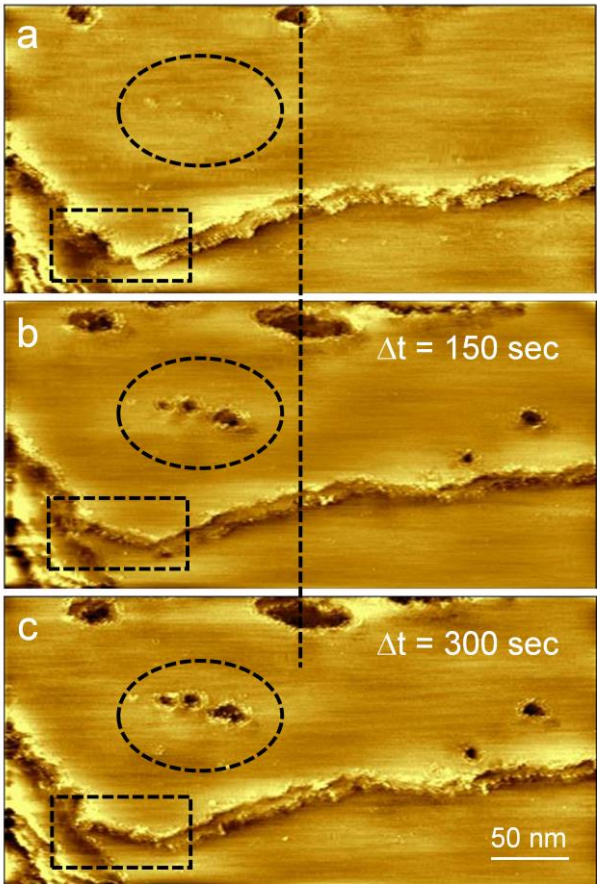

Figure 5. EC-STM images (I_{tunnel} = 0.7 nA; V_{bias} = 0.8 V) acquired on graphite in $HClO_4$ solution at V_{EC} just below 0.9 V. The acquisition time of each image (panels a, b and c) is 150 s. The reported Δt refers to the elapsed time computed from the scanning start of the first image (a) to the scanning start of the b) (150 s) or c) (300 s) image. The formation of damages (holes) on the graphite surface is marked by dashed circles. Pre-existing damages increase their sizes (see the dashed straight line). In addition, we observe that the terrace edges are smoothed and the corner eroded, as marked by the dashed squares.

When H_2SO_4 is used as electrolyte solution, the morphology and the structure of the graphite surface follow the same evolution observed with $HClO_4$. In Figure 6a, the EC-AFM image of the blisters is reported, while the structure of the nano-protrusion is shown in the inset. The complete CV spectrum (panel b) is characterized by three anodic peaks known as intercalation stages at different depth inside the graphite[5]. In this case, we estimate that the stored charge in the sample is about three times larger than previously reported for the perchloric acid. Structures comparable

to nano-protrusions were observed on graphite surfaces when plunged in sulfuric acid after cycling the electrochemical potential several times[17]. Nevertheless, we observe these nano-protrusions also as soon as the first anodic peak (at 1.1 V) is measured, in agreement with previous results acquired with perchloric acid. Interestingly, these structures coexist with graphite terrace faceting, both of them representing a precursor stage of the blisters formation.

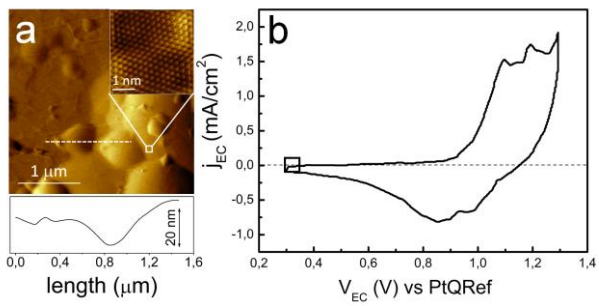

Figure 6. a) EC-AFM image (topography, contact mode) acquired on graphite immersed in 1M H_2SO_4, after several electrochemical cycles. At the bottom, scan profile of the graphite surface. *Inset*: atomic resolution of nano-protrusions found on graphite as observed by the EC-STM (I_{tunnel} = 1.0 nA; V_{bias} = 0.3 V)]. b) Characteristic CV (v_{scan} = 30 mV/s) of graphite in H_2SO_4 electrolyte. The square symbol marks the value of the electrochemical potential at which both the EC-AFM and EC-STM images (panel a) have been acquired. For the definition of the PtQRef, electrode, see caption of Figure 1.

As a final common electrolyte, we studied the graphite morphology when immersed in H_3PO_4 (see Figure 7), generally used in industrial protocols to corrode the graphite surface. Here (panel a), no blisters are observed but an enhancement of the surface roughness is measured on the nm scale by EC-AFM (compare this scan profile with the one reported in Figure 1a), when the sample V_{EC} goes beyond 1.4 V. On the other hand, it was not possible to achieve STM atomic resolution on this irregular surface. The CV (panel b) shows a single anodic peak at 1.5 V, measured only during the first (full line) potential sweep. This situation is different from what was observed in perchloric or sulfuric acid, where CV peaks related to the steps of the intercalation process are reproducible during successive scans. Apparently, after the first CV

scan in H_3PO_4, the HOPG crystal undergoes heavy processes, resulting in significant changes of the surface chemistry.

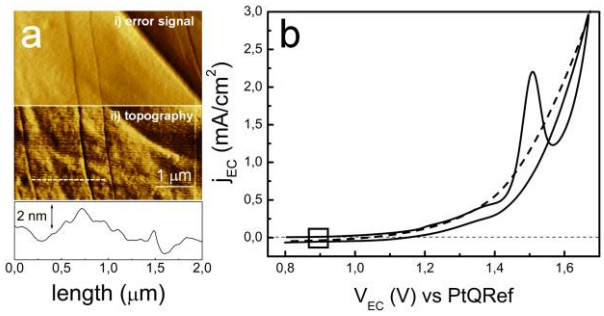

Figure 7. a) EC-AFM image [error signal (i) and topography (ii), contact mode] acquired on graphite immersed in H_3PO_4 solution, after a single electrochemical cycle. At the bottom, scan profile of the graphite surface. b) Characteristic CV (v_{scan} = 150 mV/s) of graphite in H_3PO_4 electrolyte, after a first EC cycle (full line) and a second positive sweep (dashed line). The square symbol marks the value of the electrochemical potential at which the EC-AFM image (of panel a) has been acquired. For the definition of the PtQRef, electrode, see caption of Figure1.

Conclusions.

In conclusion, the collected results cast light on the first stages of the graphite intercalation process when $HClO_4$ or H_2SO_4 are used and on their peculiar effects with respect to other electrolytes, which do not cause blisters growth. We observe a terrace faceting and the formation of small-sized (about 1 nm in diameter) protrusions. Their structure is compared to flat graphite, suggesting a C-C bond stretching not exceeding 3%. In addition, anions intercalation, which starts at defect sites, can promote the progressive damage the graphite surface (holes) within a few minutes, limiting the quality and the size of the exfoliated graphene sheets.

Within the current debate on the delamination of layered crystals, the understanding of the intercalation molecular mechanisms in graphite will increase the control and reliability of the process, improving reproducibility and opening new applications of the intercalated layers for

the production of graphene film based actuators. On the other hand, the perspective application of the developed experimental approach could allow for the understanding and comparison of exfoliation procedures carried out on different layered materials and in different electrochemical environments.

Author Information.

The authors declare no competing financial interests.

Acknowledgment.

The authors are grateful to L. Magagnin (Department of Chemistry, Politecnico di Milano), A. Picone (Department of Physics, Politecnico di Milano), S. Mertens (TU Wien), M. Sambi and L. Colazzo (Department of Chemical Sciences, Università degli Studi di Padova) for useful discussions.

References.

(1) Geim, A. K. Graphene: Status and Perspectives. *Science* **2009**, *324*, 1530-1534.

(2) Rao, C. N. R.; Ramakrishna Matte, H. S. S.; Maitra, U. Graphene Analogues of Inorganic Layered Materials. *Angew. Chem. Int. Ed*. **2013**, *52*, 13162-13185.

(3) Ferrari, A. C.; Bonaccorso, F.; Fal'ko, V.; Novoselov, K. S.; Roche, S.; Bøggild, P.; Borini, S.; Koppens, F. H.; Palermo, V.; Pugno, N. *et al.* Science and Technology Roadmap for Graphene, Related Two-Dimensional Crystals, and Hybrid Systems. *Nanoscale* **2015**, *7*, 4598-4810.

(4) Nicolosi, V.; Chhowalla, M.; Kanatzidis, M. G.; Strano, M. S.; Coleman, J. N. Liquid Exfoliation of Layered Materials. *Science* **2013**, *340*, 1226419-1(18).

(5) Feng, H.; Hu, Z.; Liu, X. Facile and Efficient Exfoliation of Inorganic Layered Materials Using Liquids Alkali Metal Alloys, *Chem. Commun*. **2015**, *51*, 10961-10964.

(6) Xia, Z. Y.; Pezzini, S.; Treossi, E.; Giambastiani, G.; Corticelli, F.; Morandi, V.; Zanelli, A.; Bellani, V.; Palermo, V. The Exfoliation of Graphene in Liquids by Electrochemical, Chemical and Sonication-Assisted Techniques: A Nanoscale Study. *Adv. Function. Mater.* **2013**, *23*, 4684-4693.

(7) Alliata, D.; Kötz, R.; Haas, O. In-Situ AFM Study of Interlayer Spacing during Anion Intercalation into HOPG in Aqueous Electrolyte. *Langmuir* **1999**, *15*, 8483-8489.

(8) Alliata, D.; Häring, P; Haas, O.; Kötz, R.; Siegenthaler, H. Anion Intercalation into Highly Oriented Pyrolitic Graphite studied by Electrochemical Atomic Force Microscopy. *Electrochemistry Communications* **1999**, *1*, 5-9.

(9) Itaya, K.; Tomita, E. Scanning Tunneling Microscope for Electrochemistry – a New Concept for the In-Situ Scanning Tunneling Microscope in Electrolyte Solutions. *Surf. Sci.* **1988**, *201*, L507-L512.

(10) Itaya, K. In Situ Scanning Tunneling Microscopy in Electrolyte Solutions. *Prog. Surf. Sci*. **1998**, *58*, 121-247.

(11) Itaya, K. Recent Progresses of Electrochemical Surface Science -Importance of Surface Imaging with Atomic Scale-. *Electrochemistry* **2015**, *83*, 670-679.

(12) Goletti, C.; Bussetti, G.; Violante, A.; Bonanni, B.; Di Giovannantonio, M.; Serrano, G.; Breuer, S.; Gentz, K.; Wandelt, K. Cu(110) Surface in Hydrochloric Acid Solution: Potential Dependent Chloride Adsorption and Surface Restructuring. *J. Phys. Chem. C* **2015**, *119*, 1782-1790.

(13) Madry, B.; Wandelt, K.; Nowicki, M. Deposition of Copper Multilayers on Au(111) in Sulfuric Acid Solution: an Electrochemical Scanning Tunneling Microscopy Study. *Surf. Sci.* **2015**, *637-638*, 77-84.

(14) Phan, T. H.; Kosmala, T.; Wandelt, K. Potential Dependence of Self-Assembled Porphyrin Layers on a Cu(111) Electrode Surface: In Situ STM Study. *Surf. Sci*. **2015**, *631*, 207-212.

(15) Gewirth, A. A.; Bard, A. J. In Situ Scanning Tunneling Microscopy of the Anodic Oxidation of Highly Oriented Pyrolytic Graphite Surfaces. *J. Phys. Chem*. **1988**, *92*, 5563-5566.

(16) Oden, P. I.; Thundat, T.; Nagahara, L. A.; Lindsay, S. M.; Adams, G. B.; Sankey O. F. Superperiodic Features Observed on Graphite under Solution with Scanning Tunneling Microscopy. *Surf. Sci. Lett*. **1991**, *254*, L454-L459.

(17) Zhang, B.; Wang, E. Effects of Anodic Oxidation on the Surface Structure of Highly Oriented Pyrolytic Graphite Revealed by In Situ Electrochemical Scanning Tunneling Microscopy in H2SO4 Solution. *Electrochimica Acta* **1995**, *40*, 2627-2633.

(18) Kovtyukhova, N. I.; Wang, Y.; Berkdemir, A.; Cruz-Silva, R.; Terrones, M.; Crespi, V. H.; Mallouk, T. E. Non-Oxidative Intercalation and Exfoliation of Graphite by Brønsted Acids. *Nature Chemistry* **2014**, *6*, 957-963.

(19) Meyer, J. C.; Geim, A. K.; Katsnelson, M. I.; Novoselov, K. S.; Booth, T. J.; Roth, S. The Structure of Suspended Graphene Sheets. *Nature* **2007**, *446*, 60-63.

(20) Fasolino, A.; Los, J. H.; Katsnelson, M. I. Intrinsic ripples in graphene. *Nature Mater.* **2007**, *6*, 858-861.

(21) Grantab, R.; Shenoy, V. B.; Ruoff, R. S. Anomalous Strength Characteristics of Tilt Grain Boundaries in Graphene. *Science* **2010**, *12*, 946-948.

(22) Rasool, H. I.; Ophus, C.; Klug, W. S.; Zettl, A.; Gimzewski, J. K. Measurements of the Intrinsic Strength of Crystalline and Polycrystalline Graphene. *Nature Comm*. **2013**, *4*, 2811(1)-2811(7).

(23) Zamborlini, G.; Imam, M.; Petra, L. L.; Mentes, T. O.; Stojić, N.; Africh, C.; Sala, A.; Binggeli, N.; Comelli, G.; Locatelli, A. Nanobubbles at GPa under Graphene. *Nano Lett.* **2015**, *15*, 6162-6169.

(24) Goss, C. A.; Brumfield, J. C.; Irene, E. A.; Murray, R. W. Imaging the Incipient Electrochemical Oxidation of Highly Oriented Pyrolytic Graphite. *Anal. Chem*. **1993**, *65*, 1378-1389.

TOC GRAPHICS

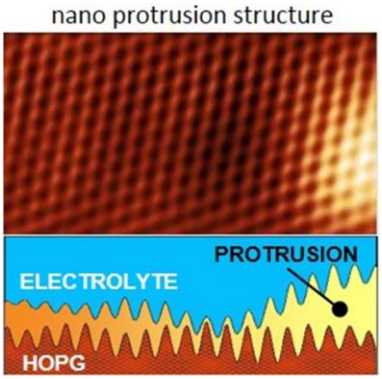

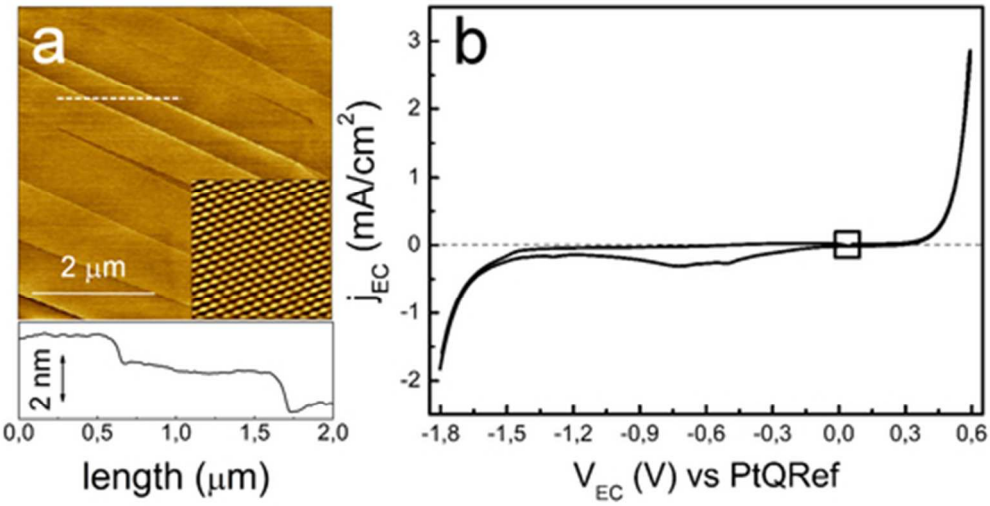

Figure 1. a) EC-AFM image (topography, contact mode) acquired on graphite immersed in HCl solution, after several electrochemical cycles. The atomic resolution [EC-STM (I_{tunnel} = 2 nA; V_{bias} = 0.3 V)] is reported in the *inset* (5 x 5 nm^2). At the bottom, scan profile of the graphite terraces along the white dotted line. b) Characteristic CV (scan rate v_{scan} = 100 mV/s) of graphite in HCl electrolyte. The square symbol marks the electrochemical potential (V_{EC}) value at which the EC-AFM and EC-STM images (of panel a) have been acquired. The V_{EC} value is measured with respect to a quasi-reference electrode (QRE), made of a Pt wire immersed inside the electrochemical solution, whose potential changes predictably with conditions.
42x22mm (300 x 300 DPI)

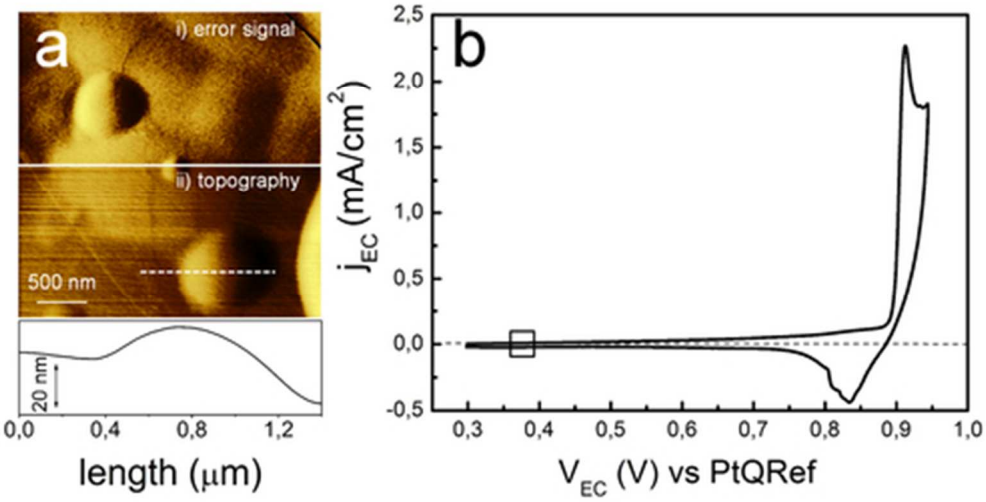

Figure 2. a) EC-AFM image [error signal (i) and topography (ii), contact mode] acquired on graphite immersed in 2M $HClO_4$ solution, after the anions intercalation and blister formation. At the bottom, scan profile of the blister. b) Characteristic CV (v_{scan} = 10 mV/s) of graphite in 2M $HClO_4$, acquired after the first sweep. The square symbol marks the value of the electrochemical potential at which the EC-AFM image (of panel a) has been acquired. For the definition of the PtQRef, electrode, see caption of Figure 1.
41x22mm (300 x 300 DPI)

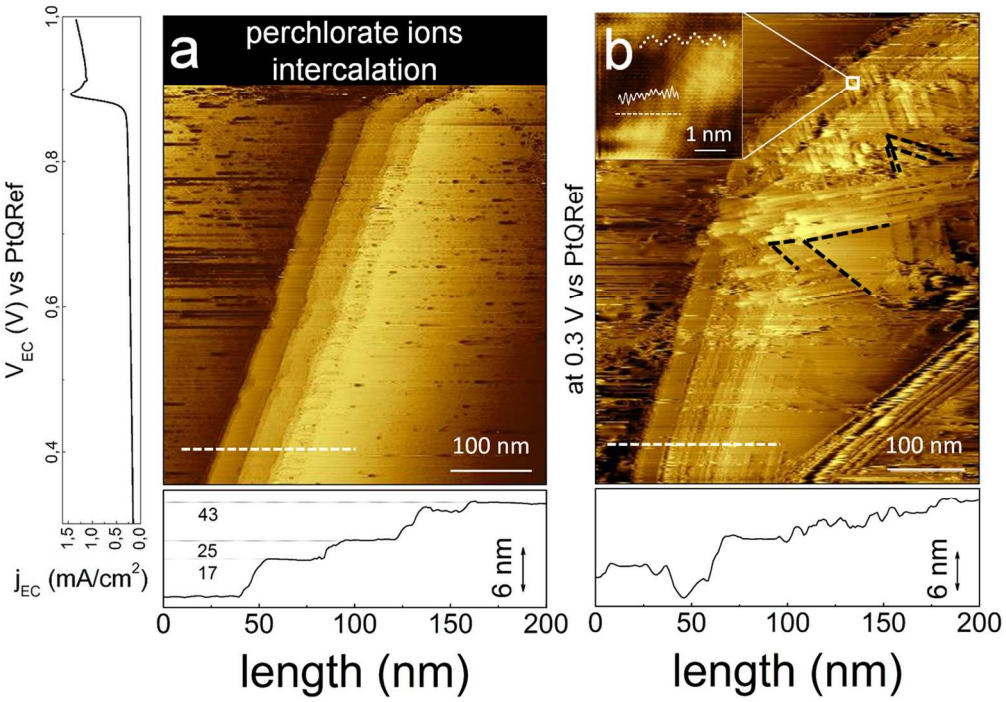

Figure 3. a) EC-STM image (I_{tunnel} = 0.2 nA) acquired on graphite immersed in $HClO_4$ solution. At the bottom, height profile of the graphite multi-atomic steps (17, 25 and 43 mono-atomic graphite layers) is reported. The graph on the left reports the CV sweep during the EC-STM scanning (see text for details). The "perchlorate ions intercalation" region takes few seconds to be covered during the completion of the bias sweep. The height profile taken along the dotted white line (bottom) shows flat terraces and sharp edges. b) EC-STM image (I_{tunnel} = 0.2 nA; V_{bias} = 0.3 V) acquired after the anions intercalation at fixed V_{EC} = 0.3 V. Preferential surface erosions, forming sharp 60° structures, are marked with black dashed lines. At the bottom, scan profile of the graphite terraces, where a significant increase of the surface roughness is observed. *Inset*: atomic resolution obtained on nano-protrusions. The dotted white line underlines the Moiré modulation super-imposed on the graphite lattice.
123x87mm (300 x 300 DPI)

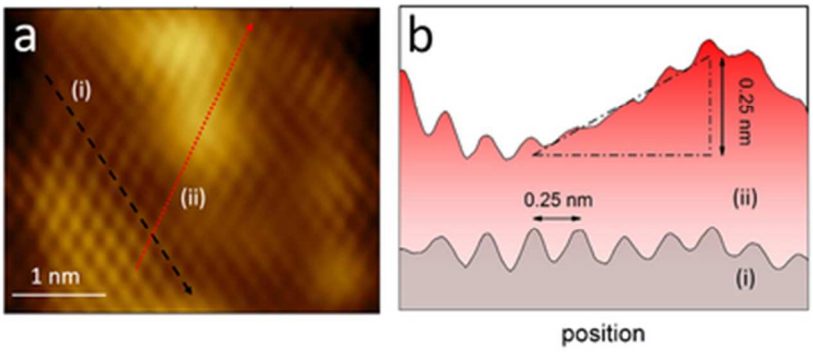

Figure 4. a) atomic resolution image of the nano-protrusion structure observed in $HClO_4$ solution [EC-STM image (I_{tunnel} = 0.7 nA; V_{bias} = 0.3 V)]. The dashed lines represent two different scan profiles: parallel to the protrusion edge [dashed black line (i)] and cutting through the swelling [dotted red line (ii)]. b) scan profiles of the nano-protrusion. The distance between two corrugation maxima is almost unaffected by the surface swelling.
35x15mm (300 x 300 DPI)

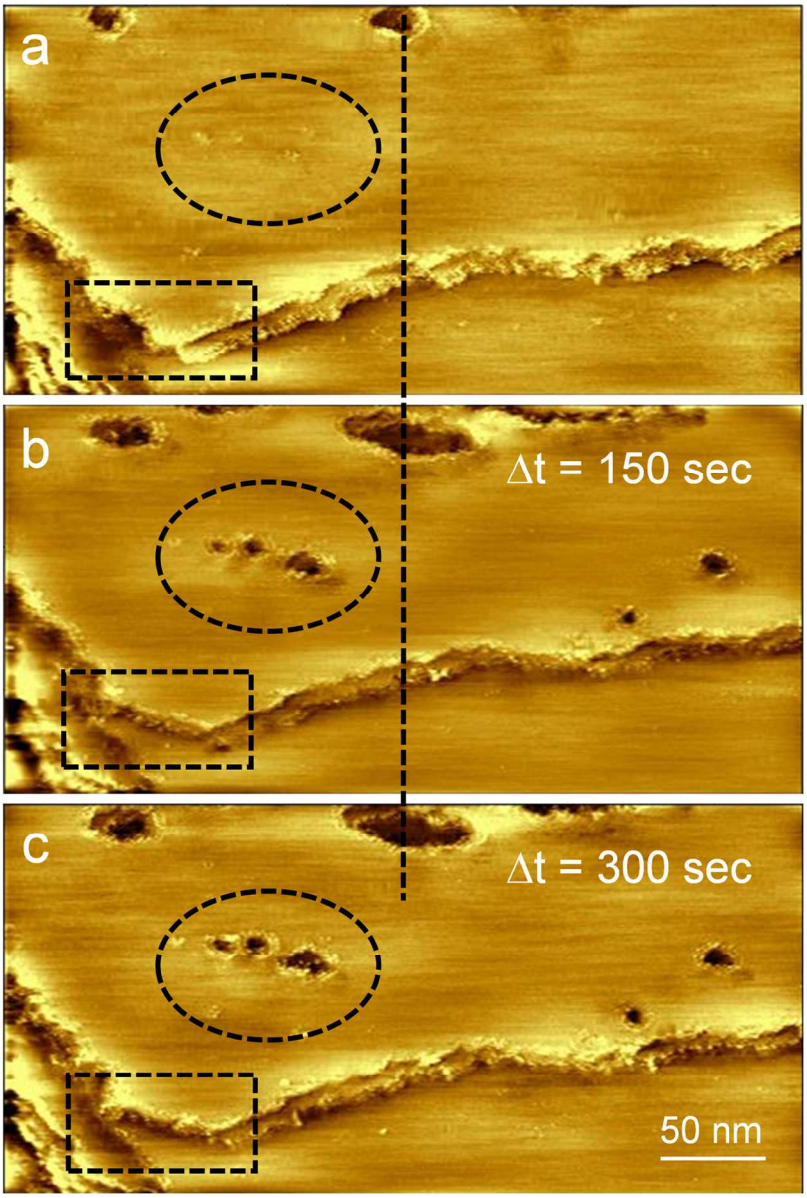

Figure 5. EC-STM images (I_{tunnel} = 0.7 nA; V_{bias} = 0.8 V) acquired on graphite in $HClO_4$ solution at V_{EC} just below 0.9 V. The acquisition time of each image (panels a, b and c) is 150 s. The reported Δt refers to the elapsed time computed from the scanning start of the first image (a) to the scanning start of the b) (150 s) or c) (300 s) image. The formation of damages (holes) on the graphite surface is marked by dashed circles. Pre-existing damages increase their sizes (see the dashed straight line). In addition, we observe that the terrace edges are smoothed and the corner eroded, as marked by the dashed squares.
117x172mm (300 x 300 DPI)

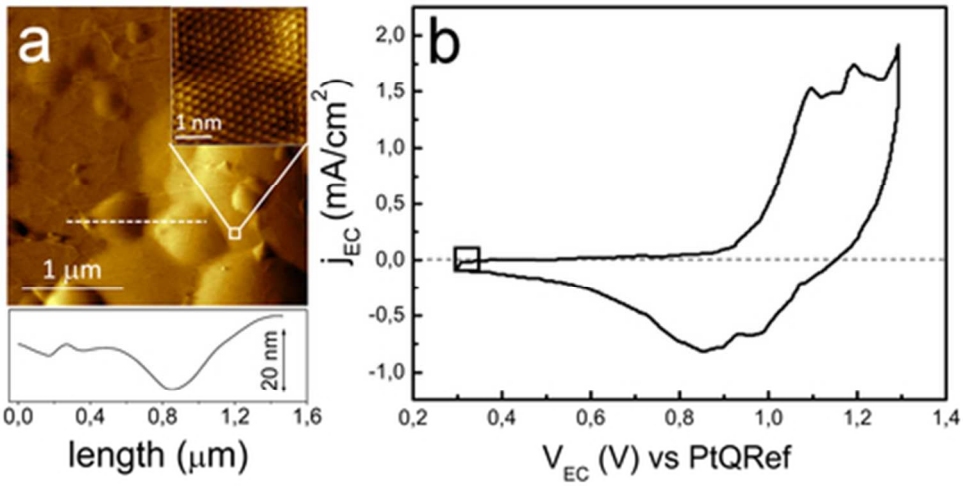

Figure 6. a) EC-AFM image (topography, contact mode) acquired on graphite immersed in 1M H_2SO_4, after several electrochemical cycles. At the bottom, scan profile of the graphite surface. *Inset*: atomic resolution of nano-protrusions found on graphite as observed by the EC-STM (I_{tunnel} = 1.0 nA; V_{bias} = 0.3 V)]. b) Characteristic CV (v_{scan} = 30 mV/s) of graphite in H_2SO_4 electrolyte. The square symbol marks the value of the electrochemical potential at which both the EC-AFM and EC-STM images (panel a) have been acquired. For the definition of the PtQRef, electrode, see caption of Figure 1.
41x21mm (300 x 300 DPI)

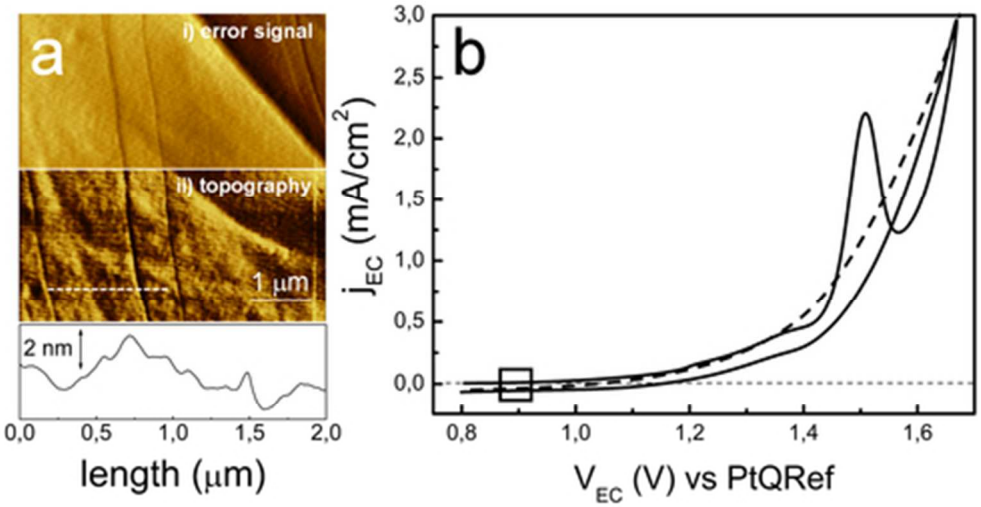

Figure 7. a) EC-AFM image [error signal (i) and topography (ii), contact mode] acquired on graphite immersed in H_3PO_4 solution, after a single electrochemical cycle. At the bottom, scan profile of the graphite surface. b) Characteristic CV (v_{scan} = 150 mV/s) of graphite in H_3PO_4 electrolyte, after a first EC cycle (full line) and a second positive sweep (dashed line). The square symbol marks the value of the electrochemical potential at which the EC-AFM image (of panel a) has been acquired. For the definition of the PtQRef, electrode, see caption of Figure 1.
41x21mm (300 x 300 DPI)

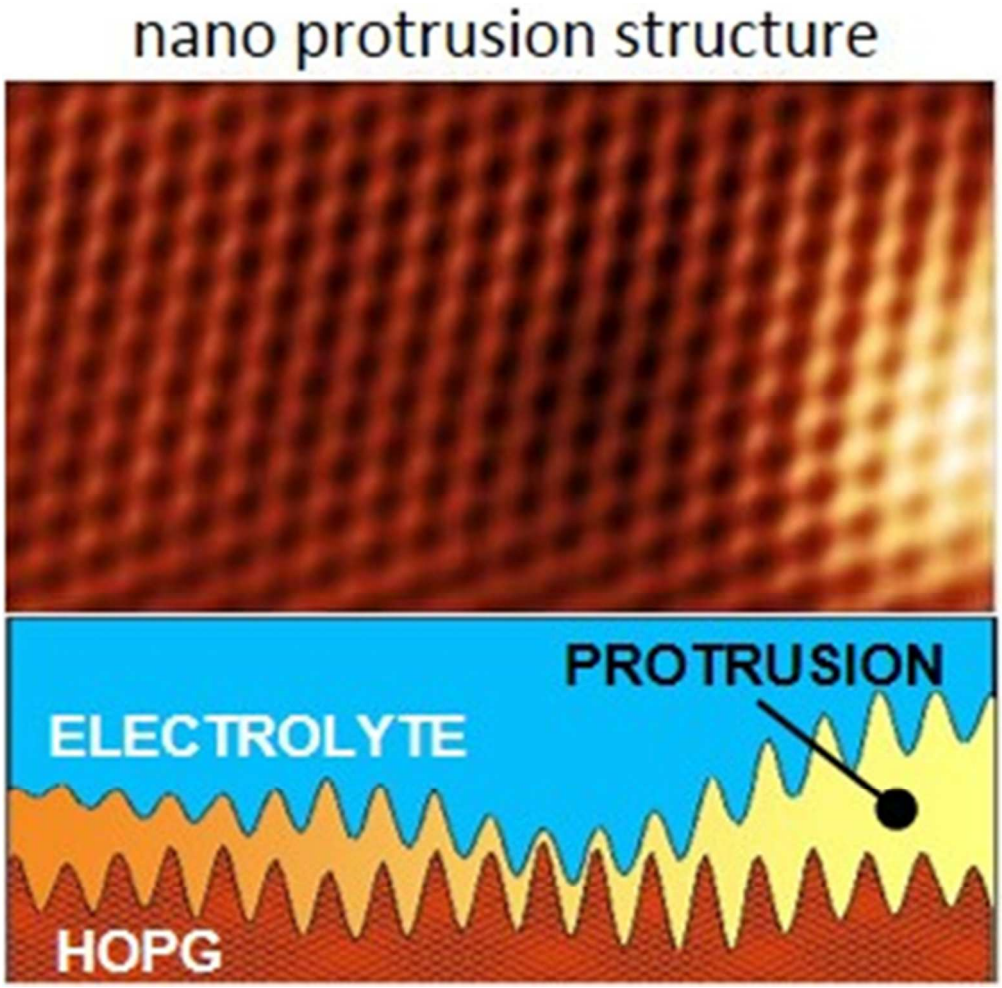

TOC
49x48mm (300 x 300 DPI)